Australian Government
Department of Defence
Defence Science and
Technology Organisation

Optimisation and Validation of the ARAMIS Digital Image Correlation System for use in Large-scale High Strain-rate Events

Vanessa Pickerd

Maritime Division
Defence Science and Technology Organisation

DSTO-TN-1203

ABSTRACT

This document provides an overview for the optimisation of the ARAMIS v6.3.0 Digital Image Correlation system (GOM mbH, Germany) for use in a large-scale, high strain-rate synergistic blast and fragmentation event. The ARAMIS system uses 3D digital photogrammetry to track surface deformation of an object during an event and produces the resultant strain data. This document highlights some key considerations for use of high-speed photogrammerty for synergistic events, not fully covered by the hardware and software manuals or literature.

RELEASE LIMITATION

Approved for public release

Published by

Maritime Division
DSTO Defence Science and Technology Organisation
506 Lorimer St
Fishermans Bend, Victoria 3207 Australia

Telephone: 1300 DEFENCE
Fax: (03) 9626 7999

AR-015-700
August 2013

APPROVED FOR PUBLIC RELEASE

Optimisation and Validation of the ARAMIS Digital Image Correlation System for use in Large-scale High Strain-rate Events

Executive Summary

The ARAMIS Digital Image Correlation system (GOM mbH, Germany) was acquired by the Defence Science and Technology Organisation for the evaluation of full-field surface strain in large-scale, high strain-rate synergistic blast and fragmentation events. The ARAMIS system uses digital images recorded at set time intervals during a deformation event to determine the surface deformation and strain of a target over time.

Due to the complexity of large-scale, high strain-rate events with high dynamic loading, optimisation of the ARAMIS system was required. Experiments were performed to determine the optimal set-up configuration for large-scale, high strain rate events and confirm that the required experimental modifications did not affect the results. This included assessing the use of high-speed cameras, mirrors, large-stand off distances and lighting. The outcomes of these experiments are detailed in this report along with recommendations and the final set-up configuration for the large-scale, high strain-rate events.

Validation of the ARAMIS system was performed by comparing the accuracy of the ARAMIS strain evaluation against a tri-axial strain gauge. An aluminium tensile sample loaded to failure in a tensile test machine was used to perform this validation. The results showed good correlation between the ARAMIS strain values and the strain gauge values in both the x and y directions.

This page is intentionally blank

Author

Vanessa Pickerd
Maritime Division

Vanessa has a Bachelor of Aerospace Engineering (BAeroEng) Degree with Honours, received from Monash University in 2010. In 2010, Vanessa joined Maritime Platforms Division (now Maritime Division), Defence Science and Technology Organisation (DSTO), where her research interests have included maritime platform survivability modelling and assessment, specifically pertaining to blast and fragmentation modelling and systems vulnerability assessment. Vanessa's current role is as a maritime platform vulnerability analyst.

This page is intentionally blank

Contents

This page is intentionally blank

1. Introduction

Conventional methods of determining the strain on a material under loading generally consist of localised strain measurements from devices such as strain gauges. When a full field strain profile is required a technique called 'digital image correlation' (DIC) provides a solution. Since the development of DIC in the 1980s [1] its use for displacement and low strain-rate calculations has become common for material testing and model validation [2, 3]. Other strain and displacement techniques such as single-point deflection histories or post deformation analysis are inadequate for model validation. The full-field nature of DIC enables large data capture and accurate model validation.

DIC in three dimensional (3D) analyses uses photogrammetric techniques to determine the full field (and localised) strain of an object. A pattern printed onto the surface of the object undergoing deformation is used to determine the displacement under loading with time. This displacement is then used to calculate the surface strain on the object. The technique requires the use of images taken in sequence over a period of time [4]. For 3D correlation the system requires two sets of images of the target taken from separate camera angles. A system calibration is required to determine the 3D space where the event occurs. This is then used to correlate the images for the determination of deflection and strain [5].

DIC has been used extensively for small scale deformation events and strain measurements in microstructures [6, 7, 8]. The majority of these events are conducted in a laboratory environment [9, 10]. The target area analysed through DIC is generally small (millimetres or centimetres) and the setup used requires a small stand-off distance [11]. Due to this, DIC is well understood for material testing in controlled laboratory situations at low frame rates [12, 13]. DIC has also been used with success in underwater experiments [14], at elevated temperatures [15] and for shock analysis [16].

Since the advancement of high-speed cameras in recent years the understanding of the use of DIC in high-speed events such as blast and ballistic impact has increased. Examples include buried blast loading [17]; ballistic impact testing [18]; shock tube analysis; and air blast [10]. Although some of these events have been performed in an outdoor setting [11], the majority were performed in a laboratory with controlled lighting and weather conditions at relatively small stand-off distances (less than 2 m).

The purpose of this paper is to investigate the issues associated with the use of DIC to capture the deformation and strain of a blast and fragmentation event in a large-scale, high strain-rate field trial. Although the use of DIC for ballistic impacts and blast has been documented [19], these events involved only blast or only projectiles. There is currently no available literature covering the use of DIC in a synergistic blast and projectile event.

This paper outlines the experimental setup requirement for the use of DIC in synergistic blast and fragmentation events with a large stand-off distance. The DIC software used for these events is the ARAMIS v6.3.0 (*GOM mbH, Braunschweig, Germany*) non-contact optical strain measurement system. The procedures and parameters that need to be considered, in addition to those provided in the ARAMIS manuals and online help, to establish the system to be used for a large-scale, high strain-rate event are outlined.

2. ARAMIS DIC System Background

DIC systems (operating in both 2D and 3D events) use a series of sequential digital images to determine the surface deformation and surface strain of objects. The systems identify features of an object and track the relative movement of those features throughout the sequential images.

The ARAMIS DIC system uses a random speckle pattern applied to the surface of the target object to create the unique features identifiable to the system. To identify these features each image is divided into an overlapping grid of facets and each facet must be unique from its neighbouring facets. Further information on facets is included in Appendix A.

To determine surface displacement of the target object each facet is tracked from one image to the next, creating a series of data points, which are mapped to create the displacement field. For 3D displacement two views (left and right) are required for each time step. The corresponding facets from the left and right image are identified in each image in the series, as shown in Figure 1. The same facet is shown in each image in Figure 1, shaded green and highlighted by a red arrow. The specimen deformation is mapped by the changing orientation and shape of the facet.

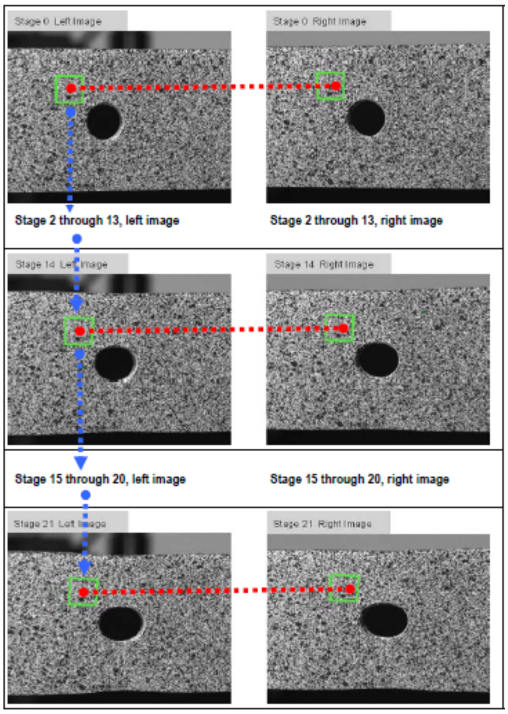

Figure 1: A set of three left and right target object images in series for use in 3D ARAMIS analysis showing the facet identification in both the left and right images, and subsequent images [20].

Prior to analysis system calibration is required. Calibration produces an operational area (for 2D events) or volume (for 3D events) in which the event can be accurately measured. Calibration is performed by moving a calibration object through a set range of motions within the area or volume where the event is to occur. Figure 2 shows the two variants of calibration objects used with the ARAMIS system, the calibration plate and the calibration cross. The calibration object chosen depends on the target area being analysed. The calibration objects and the range of motions for calibration are defined in the ARAMIS hardware manual Section 9, [21].

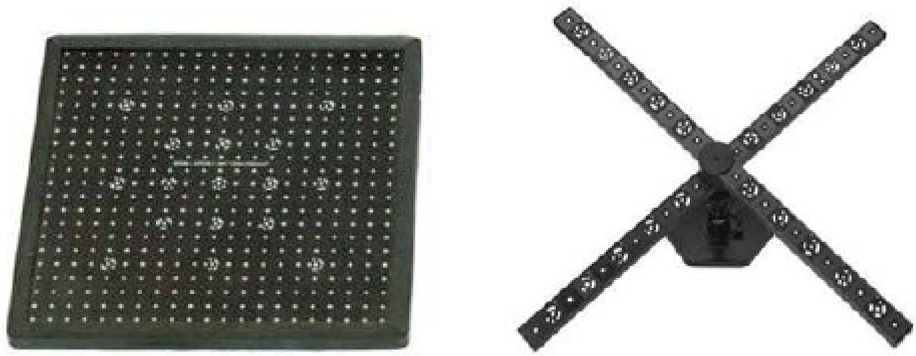

Figure 2: Calibration objects used in ARAMIS calibration, the calibration plate (left) which comes in various sizes, and calibration cross (right) [21].

Each calibration object is marked with unique points, which the ARAMIS system identifies at each orientation, to map the event volume. Information on calibration and use of the ARAMIS system is provided in the GOM user manuals [20, 21].

2.1 DIC verification in small-scale, low speed application

Validation experiments were undertaken to commission the ARAMIS software prior to use in the large-scale blast and fragmentation trial to be conducted by DSTO. A tensile test on an aluminium sample was performed and the results of the ARAMIS strain analysis were compared with strain gauge results, to verify the accuracy of the ARAMIS system in measuring strain from an image series. Similar validation work on DIC systems has been performed in the past by Tong [25]. This validation also enabled familiarisation with the ARAMIS analysis program.

The aluminium specimen used for the validation test had the dimensions of 100 mm x 200 mm (W/L) with 1 mm thickness. The specimen had three drilled holes located along the central vertical axis as shown in Figure 3. The diameter of the central hole was 3 mm. The diameter of the other holes was 5 mm. A tri-axial strain gauge was located 25 mm to the left of the central hole (on the reverse side of the specimen to that shown in Figure 3). The tensile testing was performed in a 100 kN Instron machine.

The surface of the aluminium shown in Figure 3 was analysed by the ARAMIS system. The speckle pattern, seen in the image, was applied with canned spray paint as described in Appendix A, Section A.5. The aluminium specimen already had a painted black surface

so the speckle pattern was applied using white spray paint. Ideally a white base paint would be used with a black speckle pattern, as black paint has a greater hiding power[1] than white paint; however the white speckle pattern proved acceptable in this case. The tri-axial strain gauge was applied to the back surface and the location of the strain gauge is indicated by the white rectangle in Figure 3.

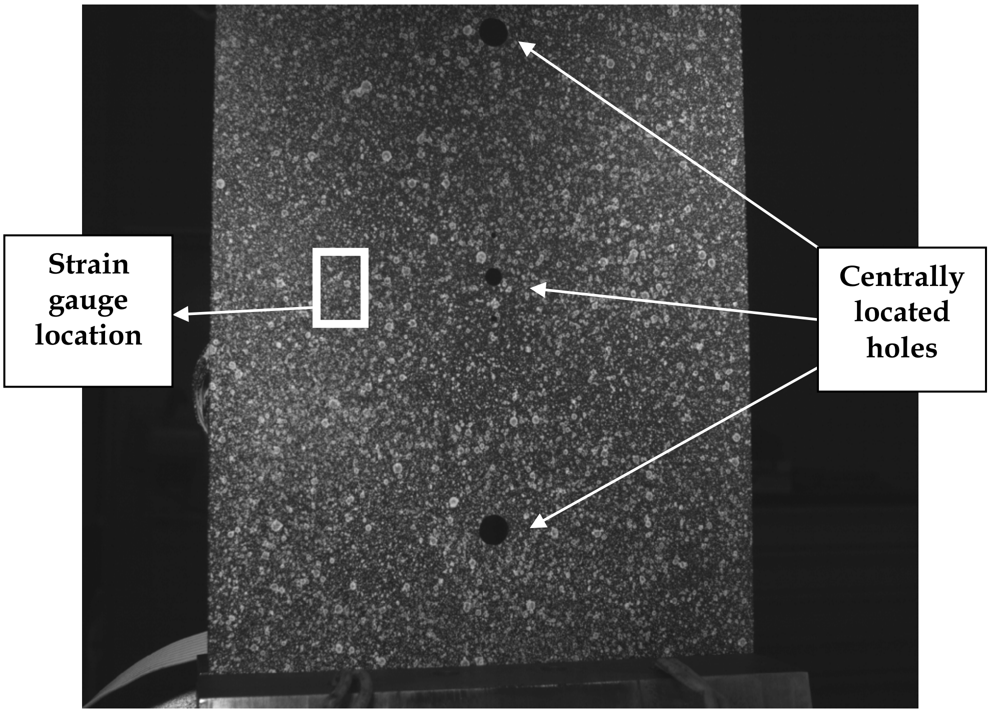

Figure 3: Image of aluminium specimen showing three holes; the strain gauge location; and speckle pattern. This image was processed in ARAMIS for determining full field strain.

The ARAMIS camera system was setup following the guidelines in the ARAMIS hardware manual [21]. The 50 mm (GOM mbH) lenses were used and the angle between the two cameras was 25.5°. Calibration of the ARAMIS system for the setup described required use of the 140 mm x 170 mm calibration plate. The calibration deviation (or calibration error) determined by the ARAMIS system was 0.071 pixels. This calibration deviation was within an acceptable range and resulted in a successful calibration. The determined measuring volume was 55/45/30 mm (Height/Width/Depth).

The laboratory where the tensile experiment was conducted did not provide adequate light for the ARAMIS system. Additional halogen lighting was used to illuminate the sample. Halogen lighting produces a high heat output which heats the sample and can also heat the cameras. The halogen lights were turned off to prevent overheating when calibration and testing were not being performed. Schmidt et al. [11] makes recommendations on the lighting used in laboratory environments.

[1] Hiding power is an optical property which measures the ability to obscure a background of contrasting colour.

The validation of the ARAMIS system experiment was performed by loading the specimen in tension until failure, which occurred at 28 kN. The tensile specimen was loaded in increments of 2 kN, and an image was recorded with the ARAMIS system using the manual acquisition method at every 2 kN increment. This resulted in a 14 stage ARAMIS file.

Comparison of the ARAMIS strain data to the measured strain gauge data was performed using equivalent strain gauge data points selected in the ARAMIS program. Two points were selected on the strain field in the ARAMIS program, in both the x and y direction. These points approximated the strain gauge location on the specimen.

The full-field ARAMIS strain results and the location of the approximated strain gauge in the y-direction (depicted by the red vertical line as applied in the ARAMIS program) is shown in Figure 4. Figure 5 shows the full-field ARAMIS strain results and the location of the approximated strain gauge in the x-direction (depicted by the red horizontal line). The strain was determined based on the displacement of the two points that make up the line, for both the x and y direction. The strain values at each stage were used to create a strain curve.

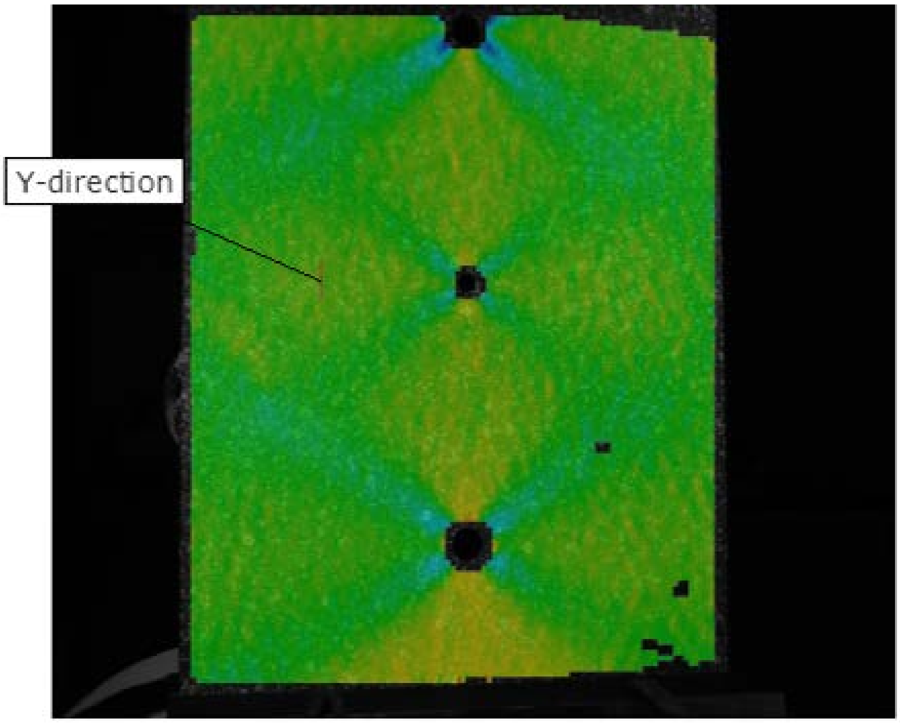

Figure 4: Aluminium tensile specimen with ARAMIS full field strain overlayed and representative strain gauge in y-direction

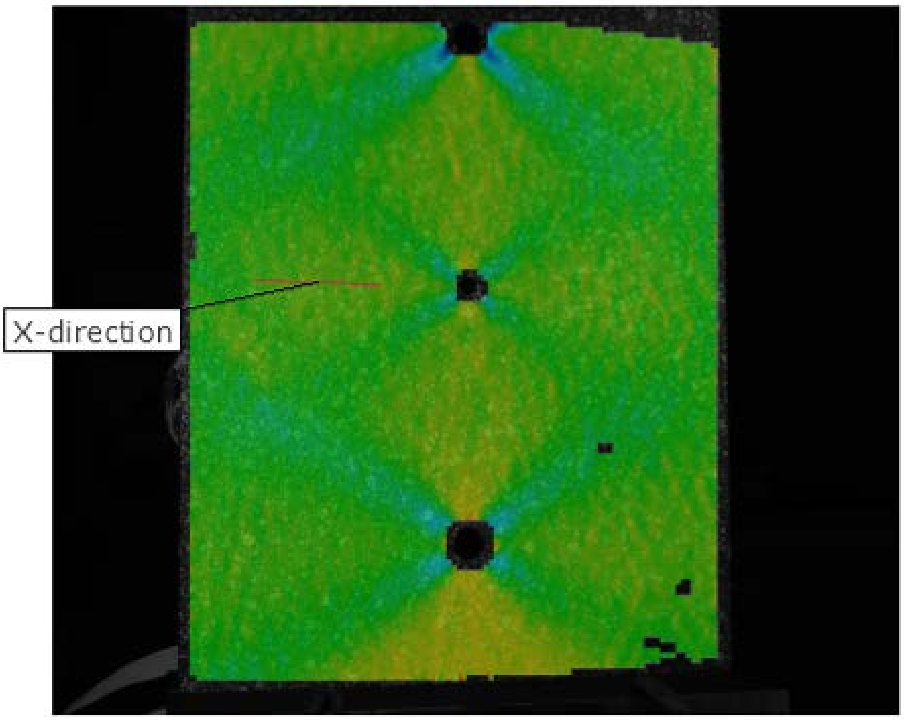

Figure 5: Aluminium tensile specimen with ARAMIS full field strain overlayed and representative strain gauge in x-direction

The results for the y and x directions from the ARAMIS equivalent strain gauge compared with the actual strain gauge are presented in Figure 6 and Figure 7, respectively. The results in the y-directions show excellent correlation.

The results in the x-direction show good correlation between the ARAMIS determined strain values and the measured strain gauge values. The small differences between the ARAMIS curves and the strain gauge curves could be a result of the approximation used to create the ARAMIS equivalent strain gauge locations. The resolution of the ARAMIS data restricts selection of the equivalent data points to a facet. This means an exact match of strain gauge location cannot always be obtained.

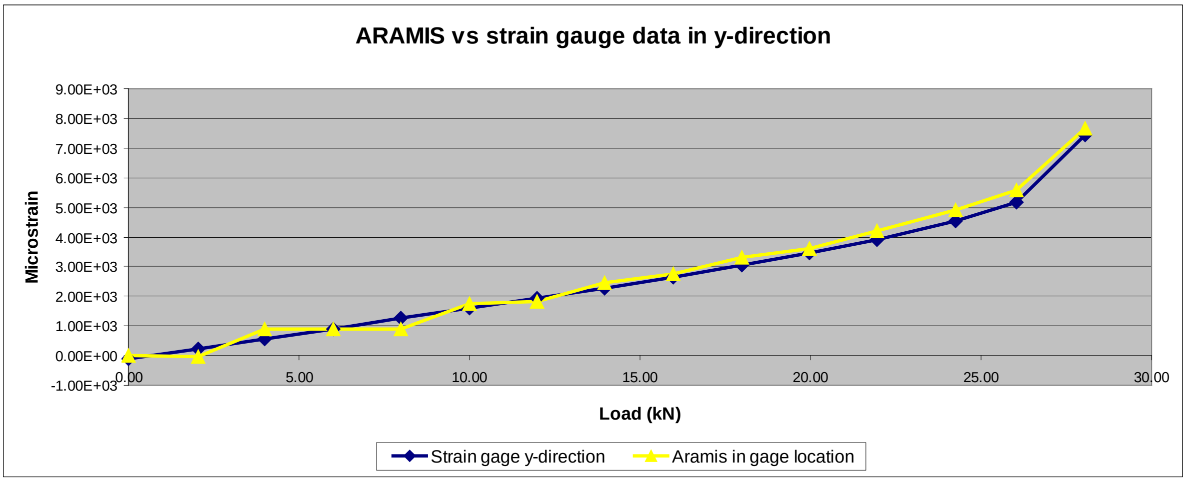

Figure 6: ARAMIS strain result in y-direction compared with strain gauge result in y-direction

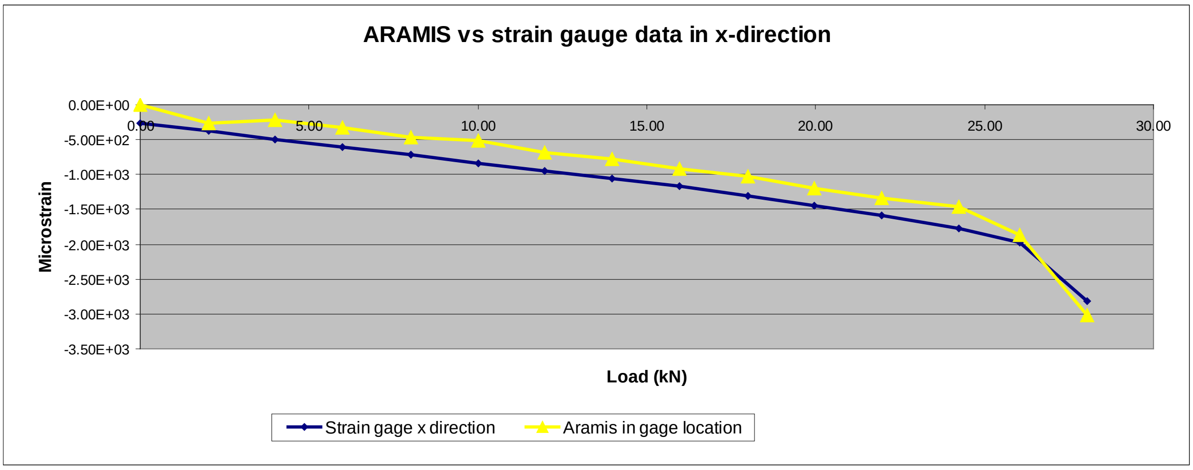

Figure 7: ARAMIS strain result in x-direction compared with strain gauge result in x-direction

3. Application in large-scale, high strain-rate events

The ARAMIS system was acquired with the objective of performing full field non-contact strain analysis on simple structures undergoing internal blast and fragmentation deformation. Before the ARAMIS system could be used for such events it had to be tested, validated and optimised for use in a high strain-rate environment. A series of tests were performed to validate the ARAMIS system for use in blast and fragmentation events.

A blast event is highly dynamic with extreme loading of the target. The introduction of fragmentation to a blast event provides added complexity including localised strain. The objective for the use of the ARAMIS system in the blast and fragmentation events was to observe the full field strain caused by blast, the localised strain caused by fragmentation and the synergistic effect of the combination of blast and fragmentation.

The main deformation in a blast and fragmentation event occurs in the first 10 ms after detonation. Measurement of the deformation and strain in such an event requires the use of high-speed video. The introduction of fragmentation to a blast event requires an increase in the safe operating distances (or stand-off distances) of equipment to that documented for a controlled blast only or ballistic impact event. Synergistic events require a specific camera setup and operational techniques not covered by the literature available for blast only or ballistic impact events, or by the ARAMIS operating manuals.

The internal synergistic blast and fragmentation event on simple structures required the detonation of both bare and fragmenting charges inside a 1 m^3 steel container. Due to the highly dynamic nature of this type of event, equipment protection was required. Protection of the high-speed cameras from fragmentation was achieved with the use of splinter-proof containers. Normally the ballistic plexiglass in a splinter-proof would be used for viewing an event; however this was not suitable for DIC images due to the low image quality obtained. Instead the cameras faced the opening of the splinter-proof containers and mirrors were used to view the event.

The layout for the DIC system in the synergistic blast and fragmentation events is shown in Figure 8. There are four high-speed cameras used in this layout (two pairs of high-speed cameras). One camera pair is focused on the flat face of the target, the other pair is focused on the edge. The flat face DIC system was used to examine how the internal loading affects the full-field strain and displacement on the surface of the flat plate; the edge DIC system was used to examine the high strain region that occurs on the edge of a welded structure.

The high-speed cameras for the DIC system were housed in open fronted splinter-proof containers orientated towards the front facing mirrors. These mirrors then reflected the target object to the cameras for image recording. The safe operating distance of the equipment is the distance from the target to the centre of a camera pair. The camera separation between the two cameras in a pair is the distance required to obtain a 25° angle between the recorded images.

The two cameras recording the edge view had a stand-off distance of 12 m and were separated by 5.6 m. The 12 m stand-off flat face view were separated by 6.5 m.

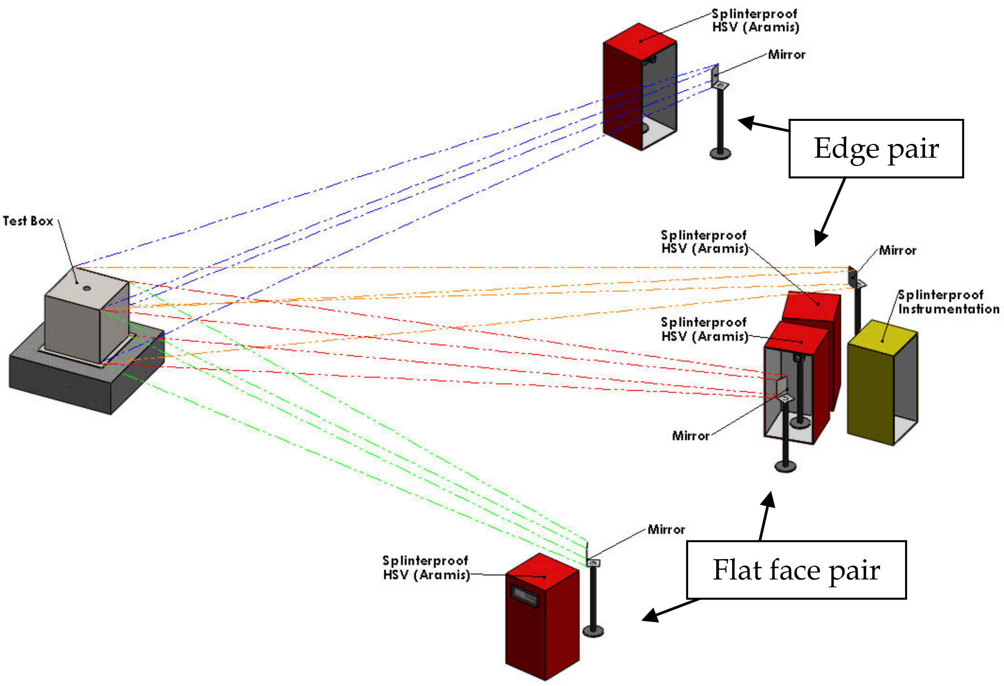

Figure 8: DIC system layout for the synergistic blast and fragmentation event

3.1 Speckle pattern

The ARAMIS system requires a speckle pattern be applied to the face of the test object. Displacement, deformation and strain are determined based on the relative movement of the speckle pattern between images. The ARAMIS program groups neighbouring pixels of the speckle pattern together to create facets, shown in Figure 9. The number of pixels in a facet is defined by the user. As each facet distorts, the amount of distortion is measured relative to the previous image, determining the displacement and strain of the material.

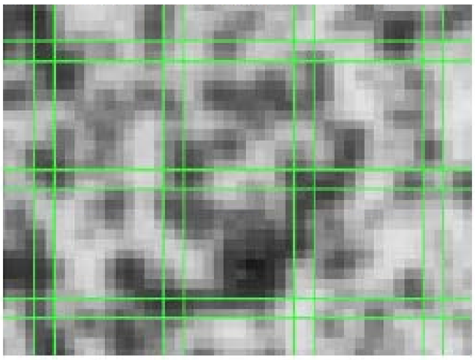

Figure 9: Facet field with overlap viewed over speckle pattern (from software user manual [20])

The number of pixels chosen for each facet determines the facet size. Smaller facets correspond to higher data resolution as each facet corresponds to a data point during

analysis. However if the facet size is smaller than ideal the facet will be indeterminable and measurement accuracy will be compromised.

The resolution of the speckle pattern applied is important as it dictates the minimum facet size that can be used. The method of speckle application affects the achievable speckle size and distribution which influences the accuracy of the deformation and strain data obtained.

Pixel	→	**Speckle**	→	**Facet**
Image dependent		Pixel and area dependent		Speckle dependent

3.1.1 Size of speckles

The minimum speckle size for system recognition depends on the resolution of the images (pixel count) and the image area [11]. The image area is comprised of the area occupied by the speckle pattern and the background. Figure 10 shows the speckle pattern on the 1 m x 1 m panel used in the blast and fragmentation event. The area inside the square contains the area for analysis. The area outside the square (highlighted red) is the background image which contains no data points for analysis.

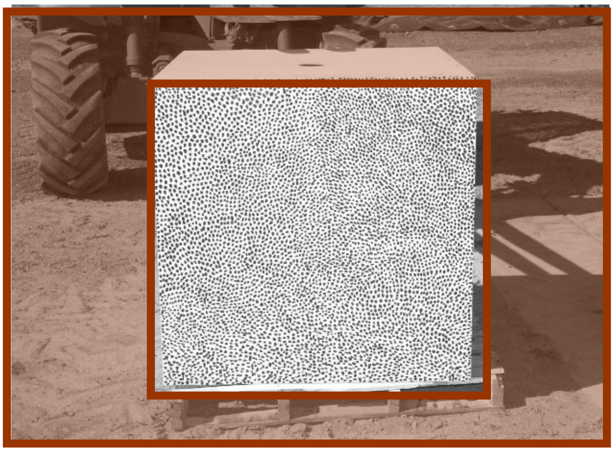

Figure 10: The speckle patterned area for data analysis is contained within the square boundary on the image. The rest of the image is the background area, highlighted red, which does not contribute data to the analysis.

For the ARAMIS system the minimum speckle size required is 5 pixels. For the large-scale blast and fragmentation event, 1024 x 1024 pixel resolution images were used at a frame rate of 7,500 fps. The total image area (speckle pattern area and background) was approximated at 1.5 m x 1.5 m. Therefore each pixel was 1500 mm divided by 1024 and had an area of 2.13 mm^2. Using the minimum pixel number of 5 for the ARAMIS system this gives a speckle area of 10.65 mm^2 or approximately 11 mm^2 as shown in Figure 11. This minimum speckle size is the smallest readable size by the software. Anything larger is acceptable.

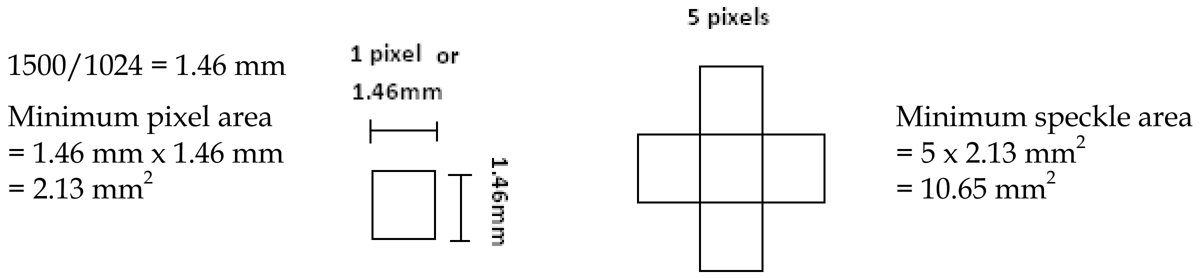

Figure 11: Average speckle size determination based on event size and image quality.

Due to the speckle application method chosen for the large-scale blast and fragmentation event the speckle size was approximately 30 mm^2, roughly three times the minimum acceptable size.

3.1.2 Consistency of pattern

It was found from DIC analysis on multiple speckle patterns, that consistency of a pattern is important for obtaining full-field results. Each facet needs to contain at least one speckle, therefore to ensure that no facets are indistinguishable and to prevent loss of data the facet size needs to be based upon the largest speckle or area of singular colour.

If the speckle pattern is inconsistent, with a few large speckles or areas of singular colour, there is a risk that there will be a loss of information. Figure 12 (a) shows a speckle pattern with too many speckles resulting in large black areas. Figure 12 (b) shows a speckle pattern with too few speckles producing large white areas. Consistency of a pattern is important to ensure that uniform data across the surface can be obtained.

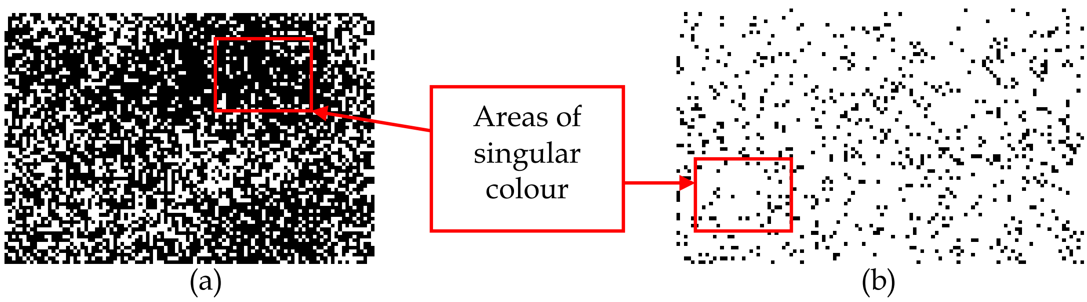

Figure 12: Examples of poor speckle pattern consistency a) too much black, b) too much white.

3.1.3 Application Techniques

To determine the most appropriate speckle pattern application technique for the blast and fragmentation event, a variety of speckle pattern application methods were trialled. The ARAMIS manual [21] describes some suggested speckle pattern application techniques.

It was determined that a tailored method of randomly applying the speckles for the large-scale experiment had to be developed. After testing a number of application techniques

the best method of application of the speckle pattern was obtained by hand painting the pattern onto the boxes, the result of which is shown in Figure 13. This method had a similar application time to the stamp method and also provided the sharpest speckle pattern (i.e. no blurred edges). The greatest number of unique data points could be achieved through this method. The drawback of this application method is that the process is labour intensive. Another option for future application is the use of a stencil pattern that can be applied to the surface.

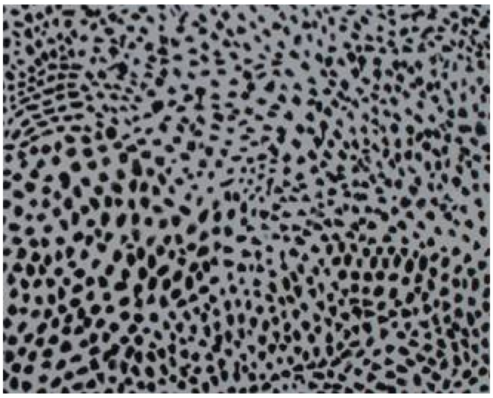

Figure 13: Pattern used on boxes from hand painting chosen as the technique to apply random speckle pattern to boxes for the blast/fragment synergy trial

3.1.4 Paint and surface treatment

From past explosive trials with internal detonations it was noted that paint applied to the surface of steel, if not treated correctly, would flake and peel off under high strain [19] [22]. This would result in a loss of data from both the loss of speckle detail on the surface and from the resulting debris travelling between the target and the camera, obstructing the images. To ensure that this did not occur in the blast and fragmentation events, the external surface of each box was grit blasted prior to painting to improve paint adhesion. The grit blasting used was approximately 60 microns. The base coating paint used was a white primer undercoat (high performance epoxy polyamide primer/undercoat [2 part], Interprotect) applied to a thickness of 45 microns[2]. The speckles were applied with commercially available matt black enamel paint. Under extreme plastic deformation, the relative deformation of the coating could cause the coating to separate resulting in loss of data.

3.2 Use of Photron high-speed video cameras in ARAMIS

The cameras used in the large-scale blast and fragmentation event for high-speed imaging were Photron SA5 cameras. These are not GOM mbH standard cameras, therefore were

[2] Details are available from the Interprotect Primer data sheet. Interprotect is made by International Paints.

not compatible with the ARAMIS image sensor controller box[3]. The images from the Photron SA5 cameras could not be read directly from the camera into the ARAMIS software for data acquisition. The images acquired using these cameras had to be loaded as an external image series into the ARAMIS software, after all images were acquired.

As the Photron high-speed cameras are not controlled by the ARAMIS controller box, the cameras must be synchronised by an external Photron system. To synchronise the cameras one camera is assigned 'master', the other 'slave'. The slave camera responds from inputs to the master camera. It is important to have the two cameras synchronised for a high-speed blast event to ensure that no deformation takes place between the left image and the right image being recorded. If a difference occurs the ARAMIS system will have difficulty aligning the facets from the left and right camera images for each image set.

When loading the calibration images as an external image series, the software requires the camera specifications. The camera specifications are entered in the 'Edit Camera' panel shown in Figure 14. The details required are the image width, image height, offset etc.

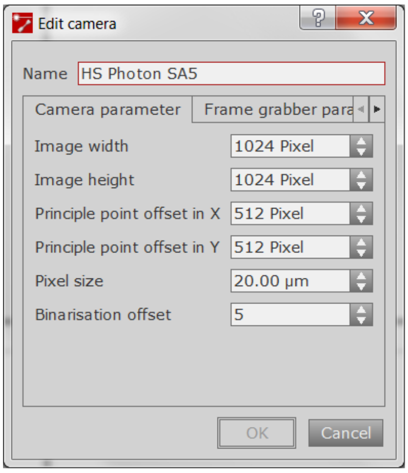

Figure 14: The 'Edit camera' panel for providing the camera specifics if not a GOM mbH specific camera

Editing the camera details can be performed from the first 'Calibration from Image Series' panel shown in Figure 15 (a).

The images taken from the left and right camera for calibration (and for the event) need to be kept in separate folders (ideally 'left images' and 'right images'). These directories are pointed to in this panel as 'Camera 1' and 'Camera 2', as shown in Figure 15 (a).

The calibration object used for calibration is selected from the second panel description, 'Calibration from Image Series', as shown in Figure 15 (b). There is an option to use instructions for calibration, but when operating using an external image series this should be turned off.

[3] The ARAMIS sensor controller box is used to control GOM standard cameras through the ARAMIS software.

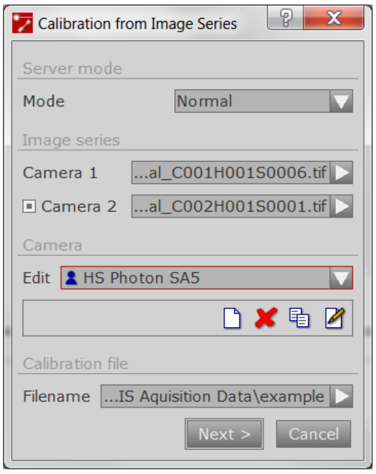

(a)

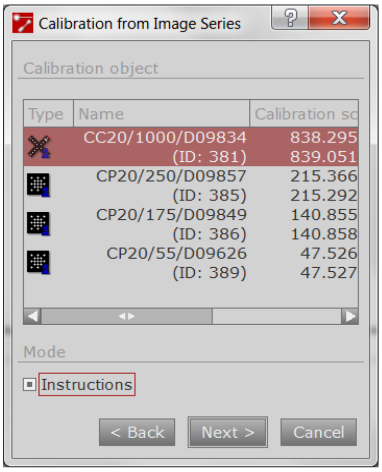

(b)

Figure 15: The 'Calibration from Image Series' panels in the ARAMIS software: a) the panel for identifying the external image series images and camera; and b) the panel for selecting the calibration object and turning off the instructions.

When setting up the cameras for image acquisition the two cameras need to be aligned so that the left and right cameras are pointing at the same location. The cross hair in the Photron software is a useful tool for alignment.

3.3 Calibration and setup distances

To protect equipment from blast waves, fragmentation and debris a safe operating distance was required for the dynamic blast and fragmentation events. An estimate of 15 m stand-off was initially used as the safe operating distance for the high-speed cameras. Calculations showed that this distance would provide an appropriate image area using 180 mm lenses as well as minimise the risk of damage to equipment from the event.

Testing was performed to check the 15 m operating distance estimate would be suitable for DIC. Before an event the ARAMIS system must be calibrated for light and depth of field. Calibration of the ARAMIS system for the large-scale blast and fragmentation events was undertaken using the calibration cross, Figure 16. The calibration process enabled verification of the appropriate operating distances for the event.

Figure 16: Calibration cross on concrete slab during explosive field trial calibration

The calibration at 15 m failed due to a 'bundle adjustment'[4] error. This indicated that the 15 m stand-off was too large. The stand-off distance was decreased to 14 m. This increased the percentage area of the image occupied by the target object. This resulted in an increased number of calibration points recognised by the system. However, not all calibration data points were recognised. For the best calibration results, all calibration data points are required. The stand-off distance was finally reduced to 12 m, which was the maximum distance at which full calibration was achieved.

3.4 Field of view limitations

Performing DIC on the edge of the target, as opposed to the flat surface, provided assessment of the edge constraints of the target undergoing internal blast pressures and associated deformation. Viewing the edge of the target with DIC introduced field-of-view restrictions due to the visualisation of each side of the edge from the opposite camera.

A feasibility study was performed to simulate the use of the ARAMIS system on an edge. The view of the ARAMIS system in this configuration was two 1 m x 1 m panels joined at a right angle to create an edge as shown in Figure 17 from the left camera view.

[4] A bundle adjustment is a ray tracing process to establish unique intersection points in the images which are used to computationally align the two cameras [11].

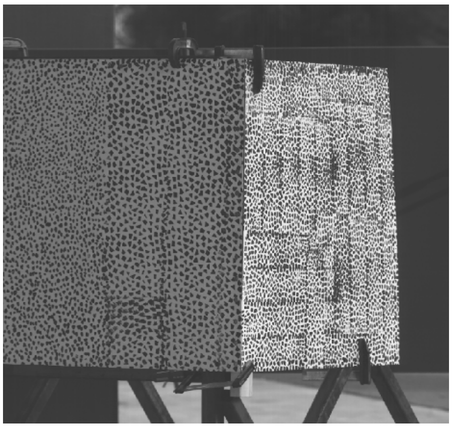

Figure 17: Left camera view of two 1m x 1m panels used to simulate the edge of a cube in pre-trial experimentation with the ARAMIS system.

One of the panels was impacted with a hammer to assess the ability of ARAMIS to determine the deformation and strain on the object for this configuration. The event was recorded with two high-speed cameras. The edge added complexity to the field-of-view by reducing the viewing area common to both cameras.

Due to the angle of the plates the ARAMIS system was unable to identify all the speckles on both sheets in each image (left and right). This is shown in Figure 18 (a) by the yellow patches highlighting the areas the ARAMIS system could not identify. The missing deflection data is visible in Figure 18 (b). Loss of speckle recognition resulted in a reduced data field. This determined that viewing the edge would not give a complete analysis of each of the flat surfaces of the box, but did give good resolution for the edge itself. Hence the requirement of four high-speed cameras for these events: one pair for the flat panel view; and one pair for the edge view.

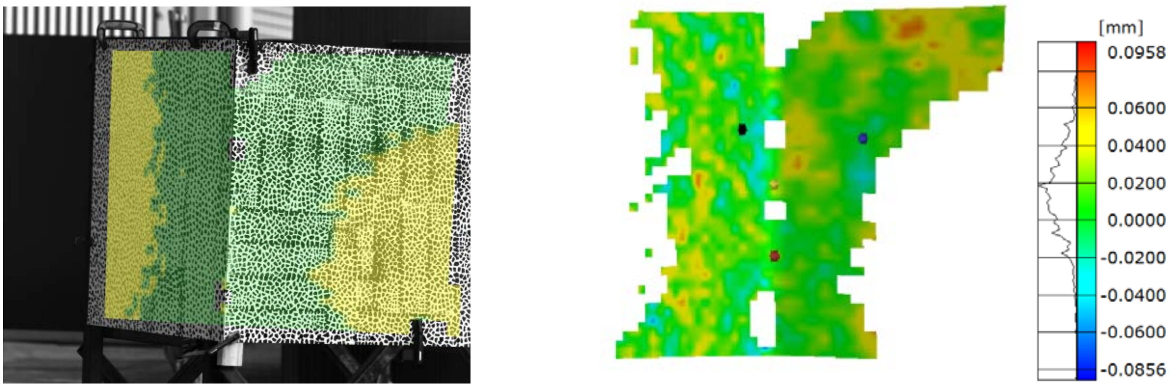

(a) (b)

Figure 18: a) Right camera view of two 1 m x 1 m panels used to simulate the edge of a cube in pre-trial experimentation. The yellow area indicates the speckles which are not identified by the system; b) the resulting ARAMIS deflection data from the test.

3.5 Camera protection and the use of mirrors

Due to the highly dynamic nature of blast and fragmentation from the detonation of the weapon in the blast and fragmentation events, protection of the cameras was essential. One of the methods for protecting the cameras was to have as much distance between the cameras and the event as possible.

The largest lenses available for use in the blast and fragmentation events were 180 mm lenses. The maximum distance that could be achieved with these lenses and still produce quality images for data analysis was 12 m (see section 3.3). The cameras were housed in open splinter-proof containers. The splinter-proof plexiglass was not used due to image distortion. Instead mirrors were used to reflect the image from the event to the protected cameras.

Protecting cameras from a dynamic event has been achieved using mirrors at small stand-off distances and with the mirrors being protected from projectiles [11]. To ensure that good images could be obtained from using mirrors at a large stand-off distance in an exposed outdoor environment, exploratory tests were performed. These tests were to address problems occurring from mirror movement, distance, image distortion and angles of reflection. The images captured through the mirrors also need to be inverted to make the image appear as it would without a mirror.

The mirrors were secured using backing frames on tripods and positioned equidistant from the cameras. Care was taken to ensure the mirrors were level and square to the cameras i.e. not tilted. The ARAMIS system requires a camera separation of 25°. Figure 19 shows the setup of the high-speed camera contained in a splinter-proof container facing the mirror. The two cameras do not need to be on the same horizontal plane, but they must have the same target area in view.

The stability of the mirrors in an outdoor environment is important. Wind can cause the mirrors to vibrate which produces distortion in the image set when processed by ARAMIS. This will cause calibration failure or large errors in the data. To ensure the image set is free from distortion a stable mirror support base was used. When the blast wave from an explosive event reaches the mirrors, the mirrors vibrate under the loading. When this occurs the data from that point on is no longer valid.

Figure 19: Camera in splinter proof facing mirror aimed at the target

3.5.1 Noise floor

The 'noise floor' of the deflection/strain results for the ARAMIS system used in the blast and fragmentation events was determined through static testing with the desired configuration. Other experimental studies have performed this verification with different system configurations [11]. The noise floor of the blast and fragmentation event system configuration (cameras located at a 12 m stand-off distance from the target, viewed through front facing mirrors) was tested using static images i.e. images recorded with no impact event on the target.

To determine the noise floor 10 consecutive images were taken during the static event. The DIC analysis was performed on these images. Four data points were selected from the DIC results to represent the deflection of the panel. These points are referenced 0 to 3 and are shown in Figure 20, representing the displacement of each point over the 10 images.

Each strain stage on the curve represents an image set in the image series. The maximum deflection recorded from this static event over 10 stages was 0.114 mm. Other laboratory tests also reflect this value, where the baseline noise of the system was recorded to be approximately ±0.1 mm.

The 0.114 mm deflection recorded for the unloaded event can be considered the baseline noise of the system for this setup configuration. The expected displacement of the target in a blast and fragmentation event is upward of 100 mm. A 0.144 mm deflection therefore corresponds to a 0.144% error for a 100 mm displacement. This will be greater for smaller displacements.

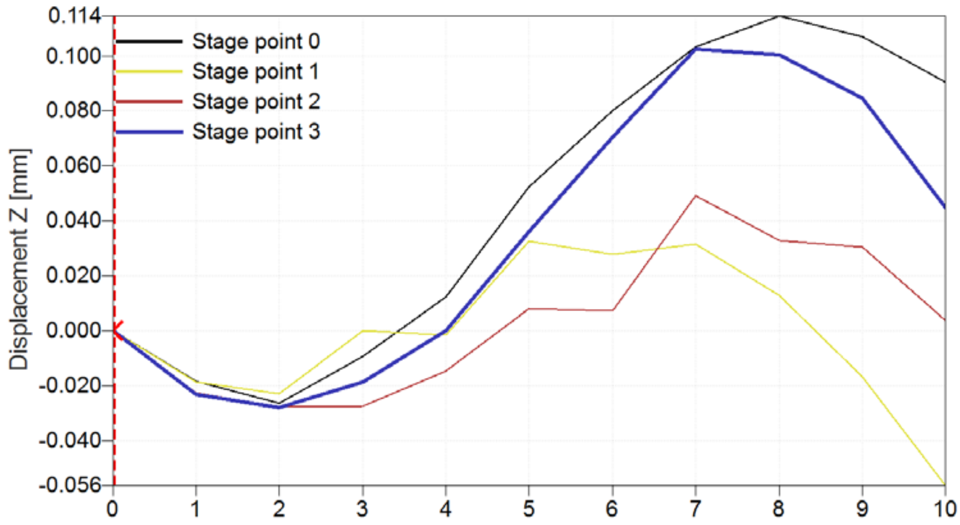

Figure 20: Graph of displacement for the undeformed panel at a 12 m stand-off viewed through mirrors. The maximum deflection is 0.114 mm for stage point 0.

3.6 Lighting

Consistent and constant lighting on the specimen during an event is required to achieve the appropriate image quality required for DIC. Testing the experimental setup for the blast fragment synergy trial in an outdoor environment identified that ambient outdoor lighting conditions provided adequate lighting for DIC, conditional that the lighting conditions between calibration and the event did not change significantly. Even overcast conditions were acceptable. The main lighting effect that influenced DIC was image contrast on sequential images.

A way of measuring the contrast of an image is to examine its luminosity (greyscale) histogram. The histogram can be used to identify the quality of contrast for the event by determining the spread of luminosity values on the histogram. If there is a good spread then the likelihood of data loss is reduced.

3.6.1 Luminosity and contrast

Luminosity is a measure of the relative brightness distribution within an image [23], taking into account that the human eye is more sensitive to green light than red or blue as shown in *equation 1* [24].

$$\text{Luminosity} = 0.3R + 0.59G + 0.11B \qquad \textit{equation 1}$$

DIC software looks at an image in greyscale to identify markers, requiring good contrast within the image. Greyscale histogram data points range between 0 (black) and 255 (white). The spread of a greyscale histogram gives an indication of the contrast of the image; if the greyscale histogram is mostly on the black side, the image is too dark; if the greyscale histogram is mostly at the white side, the image is too light.

The spread of a greyscale histogram identifies the amount of black, white and grey pixels in the image. A greater spread (e.g. 50% black, 50% white) corresponds to a better contrasting image. An ideal greyscale histogram would include only black and white values for perfect contrast, but this is unlikely in an outdoor environment. It is instead optimal to have a greater spread of values in the reference image histogram, to increase the number of reference points for the DIC software to determine the corresponding pixels in subsequent event images.

For event A1 the greyscale histogram (Figure 21) shows a spread of grey values. There is a reasonable difference between the lightest values (the peak) and the darker values. However, there are no white values in the histogram; the 159 grey value dominates, replacing white. This is acceptable as long as the darkest values and the lightest values are distinguishable. Use of the greyscale histogram prior to an event to check there is a good spread of black and white in the image helps to ensure that all data can be fully processed by the system after the event.

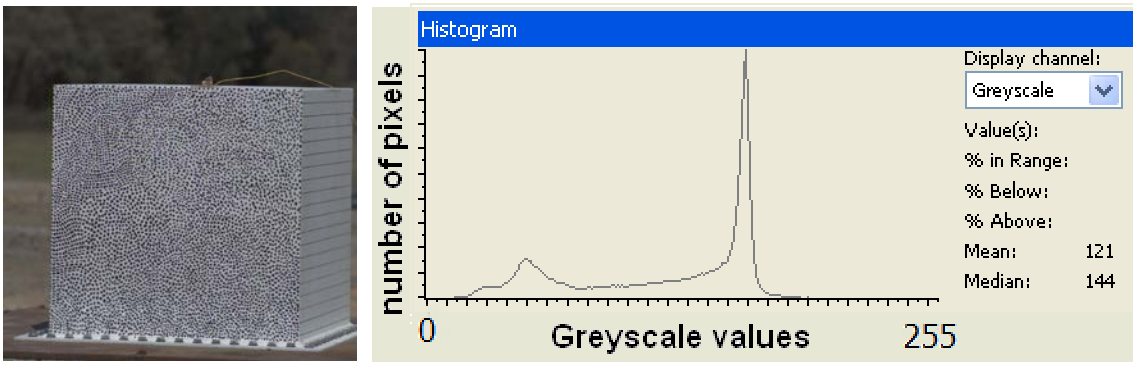

Figure 21: Image of Event A1 used to create greyscale histogram where only the speckle area is used; and luminosity (Greyscale) histogram for the speckle region of Event A1.

3.6.2 Overexposure

Overexposure of an image is a result of the presence of bright light or light reflections, which produces inconsistencies in light level across the image. There are two ways overexposure can cause data loss in DIC.

The first is overexposure in the reference image, where bright spots or reflections can appear from the image light source (artificial lighting or sunshine). One method for varying the perceived light level is adjusting the aperture of the camera. Adjusting the aperture also affects the depth of field available for the event so this should be done with caution.

Calibration of the software can be affected if overexposure occurs in the calibration images DIC may interpret reflections as data points which causes an error. If an overexposure occurs in an area that is not required for data processing, the unwanted area can be removed from evaluation by masking.

The second type of overexposure occurs from a change in light level throughout the image series. The ARAMIS program displays indeterminate areas in an image series as yellow, shown in Figure 22 (a). Any overexposure in images may cause a loss of data, shown in Figure 22 (b), where the presence of light from explosive detonation causes data loss.

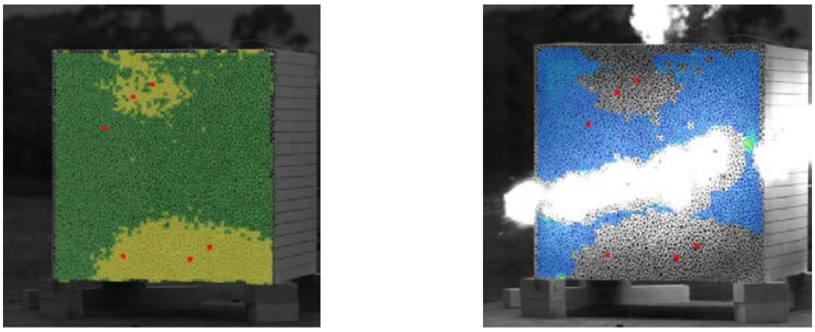

(a) (b)

Figure 22: a) Data loss displayed in ARAMIS, and b) high contrast lighting example from Blast Fragment Synergy trial

The reason for the data loss is explained by the relative luminosity between images in a series. The luminosity of the first image in the series is the reference luminosity. During the event, if the luminosity profile changes dramatically the DIC will have trouble tracking the current image to previous images and data will be lost.

In the full-field blast events this occurred in Event B2. The greyscale histogram for this event is shown for the first (reference) image, Figure 23 (a), and at 1.07 ms, Figure 23 (b). The difference between the greyscale histograms at the two time steps is significant, which resulted in a loss of data for this event. Conversely, the greyscale histograms for Event B4, Figure 24 (a) and (b), are similar for the same two time steps, so this event had minimal DIC data loss.

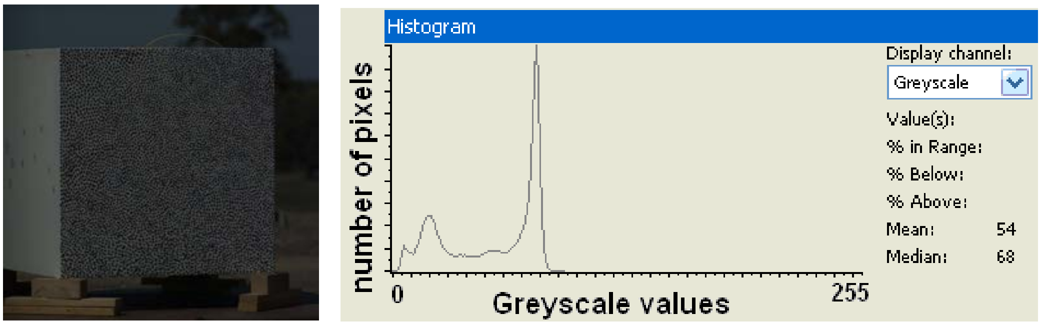

(a)

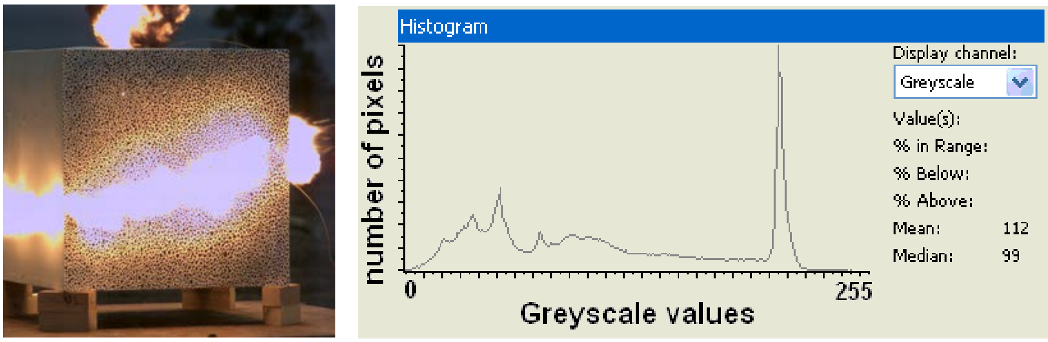

(b)

Figure 23: Event B2 image and greyscale histogram for a) reference image at time = 0 ms and b) time =1.07 ms

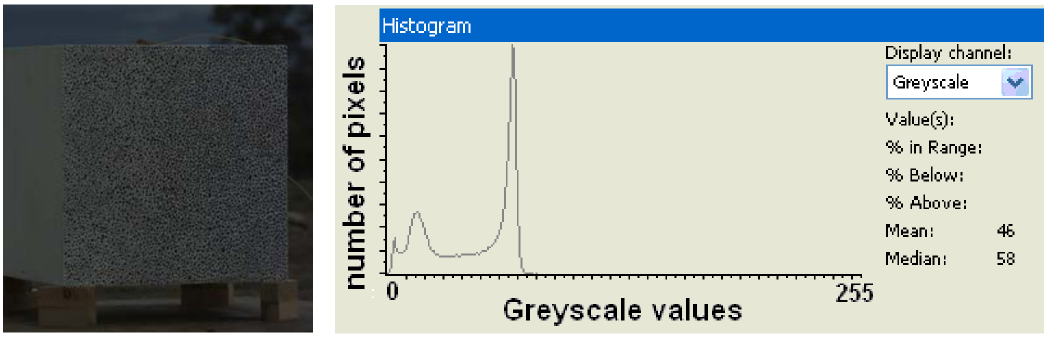

(a)

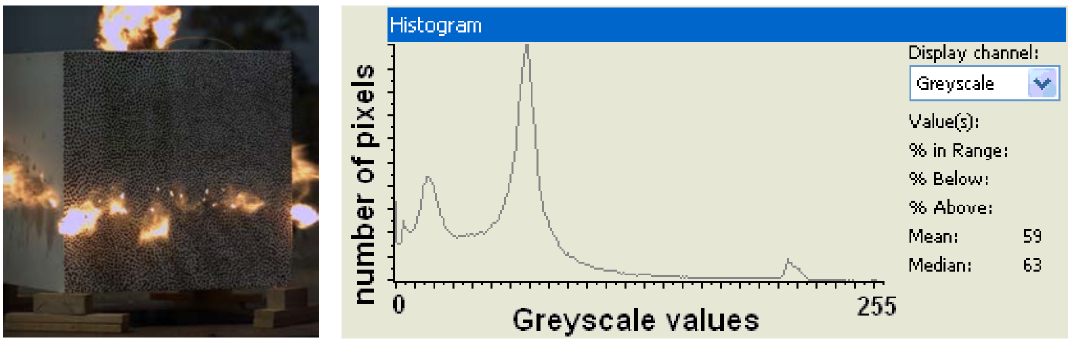

(b)

Figure 24: Event B4 image and greyscale histogram for a) the reference image at time = 0 ms and b) time =1.07 ms

To reduce the overexposure in images it is recommended to,

- Use materials with a low reflective surface
- Use matt paint on surfaces such as matt white and matt black paint
- Adjust the aperture on the camera lenses to control the perceived light level, and
- When possible reduce the light intensity.

Images taken pre-event can also be used to check the contrast of an image. If the image histogram has a good spread of values then the likelihood of data loss is reduced.

4. Conclusion

The use of DIC for full-field strain determination in ballistic impact and blast events has been well reported in literature for applications in controlled environments with single penetrators at small stand-off distances. However, these reports lack the considerations for use of DIC in synergistic blast and fragmentation events with large-stand-off distances. This report identifies and offers solutions to some of the issues associated with the use of DIC in such events.

Through a number of simulated test scenarios, the ARAMIS v6.3.0 (GOM mbH) DIC system was optimised and validated for use in large-scale, high strain-rate synergistic blast and fragmentation events. Some issues were identified with the use of the system for large-scale, high strain-rate events using high-speed photogrammetry. These issues included adequate lighting conditions, the use of mirrors, large stand-off distances, speckle pattern application and use of high-speed cameras. In each case a solution was found to optimise the system and the final setup configuration for use in synergistic blast and fragmentation events was determined.

Some of the key results from this experimental series were,

- Speckle size and application is important for high resolution results
- For highly dynamic events, paint adhesion is critical
- For 180 mm lenses the furthest stand-off distance achievable is 12 m
- Ambient lighting conditions are adequate for outdoor events
- When using mirrors in explosive events, effort must be taken to secure mirrors and avoid mirror shake
- For 3D events camera synchronisation is important
- Greyscale histograms can be used to predict image quality.

The ARAMIS system was also validated against a conventional localised strain measurement technique to determine the accuracy in strain determination. An aluminium tensile test was performed with a tri-axial strain gauge and the ARAMIS system both recording the strain output. The results showed good correlation between the two techniques.

5. Acknowledgments

I would like to thank Michael Buckland, Pat McCarthy, Alastair Douglas, Daniel Birt, Jim Nicholls (QinetiQ) and Brian Crowley (QinetiQ) for their work in commissioning the ARAMIS DIC system for use in the synergistic blast and fragmentation event series.

6. References

1. Ackermann, F. (1984) Digital Image Correlation: Performance and Potential Application in Photogrammetry. *The Photogrammetric Record* **11** (64) pp 429-439
2. Moser, R. and Lightner, J. G. (2007) Using Three-Dimensional Digital Imaging Correlation Techniques to Validate Tire Finite-Element Model. *Experimental Techniques* **31** (4) pp 29-36.
3. Bolduc, M., et al. (2008) *Improving hydrocode models using high strain rate testing*. Defence R&D Canada – Valcartier.
4. Sciammarella, C. A. and Sciammarella, F. M. (2012) Digital Image Correlation (DIC). In: *Experimental Mechanics of Solids*. John Wiley & Sons, Ltd pp 607-629.
5. Hild, F. and Roux, S. (2006) Digital image correlation: from displacement measurement to identification of elastic properties - a review. *Strain* **42** (2) 7 April 2006 pp 69-80.
6. Verhulp, E., Rietbergen, B. v. and Huiskes, R. (2003) A three-dimensional digital image correlation technique for strain measurements in microstructures. *Journal of Biomechanics* **31** 28 December 2003 pp 1313-1220.
7. Nicoletto, G., et al. (2011) Application of High Magnification Digital Image Correlation Technique to Micromechanical Strain Analysis. *Strain* **47** pp 66-73.
8. Dridi, S., Morestin, F. and Dogui, A. (2011) Use of Digital Image Correlation to Analyse the Shearing Deformation in Woven Fabric. *Experimental Techniques*.
9. Hwang, S. F., Horn, J. T. and Wang, H. J. (2008) Strain Measurement of Nickel Thin Film by a Digital Image Correlation Method. *Strain* **44** (3) pp 215-222.
10. Hargather, M. J. and Settles, G. S. (2008) Laboratory-scale techniques for the measurement of a material response to an explosive blast. *International Journal of Impact Engineering* **36** pp 940-947.
11. Schmidt, T., et al. (2004) Full-field dynamic deformation and strain measurements using high-speed digital cameras. In: *26th International Congress on High-Speed Photography and Photonics,* Alexandria, VA: September 2004, The International Society for Optical Engineering.
12. Schmidt, T., Tyson, J. and Galanulis, K. (2003) Full-field dynamic displacement and strain measurement using advanced 3D image correlation photogrametry: part 1. In *Experimental Techniques*. Wiley: pp 47-50.
13. Tong, W. (2004) Plastic surface strain mapping of bent sheets by image correlation. *Experimental Mechanics* **44** (5) May 11 pp 502-511.
14. Haile, M. A. and Ifju, P. G. (2012) Application of Elastic Image Registration and Refraction Correction for Non-Contact Underwater Strain Measurement. *Strain* **48** (2) pp 136-142.
15. Turner, J. L. and Russell, S. S. (1990) Application of digital image analysis to strain measurement at elevated temperature. *Strain* **26** (2) pp 55-59.
16. Lall, P., et al. (2009) Damage Progression Using Speckle-Correlation and High-Speed Imaging for Survivability of Leadfree Packaging Under Shock. *Strain* **45** (3) pp 267-282
17. Tiwari, V., et al. (2008) Application of 3D image correlation for full-field transient plate deformation measurements during blast loading. *International Journal of Impact Engineering* **36** pp 862-874.
18. Yu, J. H. and Dehmer, P. G. (2010) *Dynamic impact deformation analysis using high-speed cameras and ARAMIS photogrammetry software*. Army Research Laboratory.

19. Reu, P. L. and Miller, T. J. (2008) The application of high-speed digital image correlation. *The Journal of Strain Analysis for Engineering* **43** (8) 1 August pp 673-388.
20. mbH, G. (2009) *ARAMIS User Manual - Software v6.1 and higher*. Braunshweig Germany.
21. mbH, G. (2010) *ARAMIS User Information - Hardware* Brauncshweig, Germany.
22. Warden, R. (1993) *Ship Vulnerability MK 1 High Speed Cine Footage.* Defence Science and Technology Organisation.
23. McHugh, S. *Cambridge in Colour*. (2012) [Accessed 27/11/2012]; Available from: http://www.cambridgeincolour.com/.
24. Fulton, W. *A few Scanning Tips*. (2012) [Accessed 28/11/2012]; Available from: http://www.scantips.com/lights/histograms.html.
25. Tong, W. (2005) An Evaluation of Digital Image Correlation Criteria for Strain Mapping Applications. *Strain* **41** (4) pp 167-175.
26. Galanulis, K. and Winter, D. *Industrial 3D measurement Techniques*. [Accessed 2012 09/07]; Available from: http://www.gom.com/3d-software/aramis-software.html.

Appendix A: System Notes

Prior to use of the ARAMIS system, it is advisable that the DSTO Standard Operating Procedure (Appendix B), located with the ARAMIS acquisition laptop, and the ARAMIS Safety Assessment (#1997) be read. Other recommended reading includes the ARAMIS Software Instruction Manual [20] and the ARAMIS Hardware Instruction Manual [21].

A.1 Terminology

Table 1 contains a list of terms and definitions which are used throughout this report.

Table 1: Glossary of terms

Term	Definition
Pixel	The smallest single component of a digital image
Digital Image Correlation (DIC)	The use of triangulation algorithms on digital images to determine physical motion
Resolution	The number of pixels the image is comprised of
Facet	A collection of neighbouring pixels of a defined size which is required by the ARAMIS software
Facet Field	An overlapping grid pattern comprising of multiple facets
Speckle pattern	The physical pattern applied to the surface of the target for imaging

The terms pixel, facet, facet field and facet overlap are described visually in Figure 25. Figure 25 shows a black and white pattern representing an example speckle pattern, divided into pixels. Red lines indicate the facet field over the speckle pattern, which is made up of a collection on pixels. Each facet in the image is 5 pixels by 4 pixels and the facet field has a 1 pixel overlap between each facet.

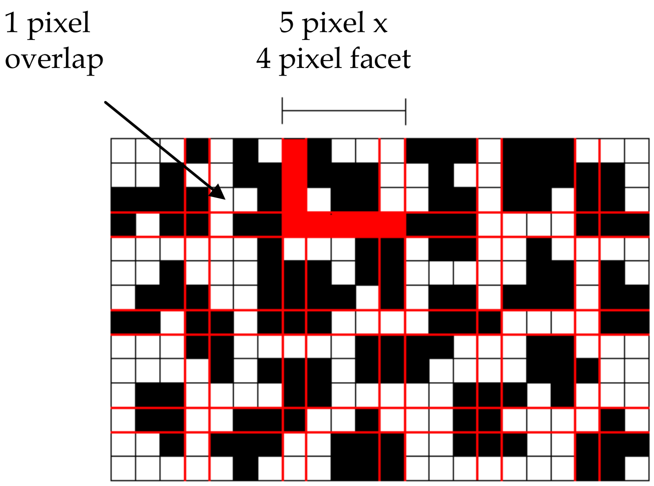

Figure 25: Pixelated speckle pattern with facet overlay in red (including facet overlap shown in solid)

A.2 Initial setup

The DSTO ARAMIS package includes the following items:

- Dell laptop with acquisition and evaluation software (Unclassified)
- Dongle licence key for laptop
- 140 x 170 mm Calibration Plate
- 55 x 44 mm Calibration Plate
- 1000 x 800 mm Calibration Cross
- Calibration plate stand
- Camera tripod with attachable camera rod
- 2 x 5M 15 Hz cameras
- 50 mm fixed focal length Lenses (includes key for changing lenses in kit)
- 12 mm fixed focal length Lenses
- Image sensor controller
- Additional items such as extension chords, lights, tool kit etc.

Before setting up the ARAMIS system the cameras best suited for the experiment need to be determined. The system operates with high-speed, low speed and thermal imaging cameras [26]. The DSTO ARAMIS image sensor controller is designed for use with low speed cameras, but the ARAMIS system can be adapted to a high-speed environment (as described in Section 3).

The basic procedure for using the ARAMIS non-contact optical measuring equipment is to use the steps outlined below.

1. Prepare the specimen with a speckle pattern (*refer to Section 3.1*)
2. Use the acquisition software license on the supplied Laptop
3. Set up tripod with camera system according to the instructions in the user manual
   - Choose appropriate camera lenses
   - Choose appropriate calibration object
   - Determine setup distance and camera separation on bar (from look up tables)
4. Connect the controller box to the cameras and the acquisition laptop
5. Place the specimen in its testing location and ensure that the lighting of the specimen is adequate
6. Focus the cameras so that images of the specimen are clear
7. Remove the specimen and follow the calibration instructions using the appropriate calibration object
8. Once calibrated replace the specimen and be sure not to touch or change the camera configuration
9. Use the desired method for image acquisition (auto or manual – manual will involve connecting the trigger button to the sensor controller)
10. Run the test
11. Prepare the images for evaluation by,
    - Using the masking tool to remove unwanted detail
    - Set an automatic start point (see Section A.4)
12. Click '*Compute Project'*

Once the images have been processed evaluation of the images can be managed on any computer using the evaluation software dongle. Use the ARAMIS software in *Evaluation Mode* to work out displacement, strain etc.

The use of ARAMIS as a 2D or 3D system is dependent on the user requirements, the set up and calibration will vary slightly between the two options. Use of the 2D system is beneficial when no out of plane motion is expected.

A.3 Calibration Setup

Before recording data the non-contact optical measuring system needs to be calibrated. The DSTO ARAMIS system comes with three calibration objects. The use of each of these objects depends on the size of the object you are testing.

Note: care must be taken when handling! *Each calibration object is specifically designed for use with the ARAMIS calibration system. The calibration objects contain markings which are recognised by the software in calibration mode. The surfaces of the calibration plate are ceramic to reduce thermal expansion effects and designed to reduce light reflections. Any fingerprints on the object's surface cannot be removed and may affect calibration results.*

To determine which board is appropriate for an experiment a table is provided in the ARAMIS hardware manual [21] (refer to Section 3.2.3 for the 5M system). This table outlines which calibration object is required to achieve a certain measured area or volume based on the lenses used. It also states the distance the calibration object should be from the cameras; and the distance between the two cameras to obtain a 25° angle at that distance. This table provides a guide for defined conditions to ensure the calibration is successful.

Ideally before calibrating, set up the test with the specimen in the conditions to be tested and the ARAMIS software should be used to check the quality of the specimen images by zooming in on the image. This includes the focus, lighting and size of the image, and the clarity of the speckle pattern. The calibration must be performed in the same conditions as the test.

Note*: Once the calibration is done, the cameras and stand-off distances cannot be changed without having to repeat the calibration process.*

Calibration is performed by placing the calibration object in front of the specimen, or if possible replacing the specimen with the calibration object, and following the instructions as described by the hardware manual [21] (Section 9 for 3D and Section 10 for 2D analysis).

A.4 Start points

If the specimen images are of good quality a start point should be achievable by clicking 'A*uto Start Point*' in the software. The start point should always be in the image frame. The start point is a facet which is present in each image at each stage. If the 'Auto Start Point'

cannot find a start point it may be that the images are not suitable and the software cannot determine the equivalent facets between one image and the next. For less than ideal images it may be necessary to increase the tolerance (*Max Deviation*) on the automatic start point for one to be found.

If a discontinuity, such as a crack, occurs through the object separating speckle pattern, then the strain data will only be calculated for the area that contains the start point. An additional start point can be made on the remaining speckle pattern to ensure that data is calculated. If the image quality is poor in a region, resulting in data loss, adding multiple start points in the region can resolve the data. If extra start points are required then selecting a start point manually can be done using 'A*dd Start Point*'. A start point can be selected from the first image and then checked for compatibility through the rest of the series of images.

A start point can also be selected manually for each image by selecting the desired facet to become the start point (the same facet needs to be selected in both left and right images for 3D) and then manually locating the selected facet in all subsequent images.

A.5 Speckle pattern application for small targets

A method for speckle pattern application on small surface areas, as suggested in the GOM mbH user manuals, is canned spray paint. This spray paint application technique is appropriate for small samples due to the size of the speckles created. The ARAMIS user manual provides a speckle size guide for spray paint application.

When using canned spray paint partially pressing the trigger reduces the flow and smaller speckles can be achieved. Not pressing the trigger sufficiently may cause the nozzle to leak which will produce an undesirable amount of paint.

The use of spray paint should be performed in a fume cupboard or well ventilated space. Initial experimentation using the canned spray paint showed that the application should be started away from the sample (to avoid droplets until the correct pressure is being applied) and then smoothly moved across the sample surface. The application can be repeated until the desired speckle pattern is achieved.

Appendix B: Standard Operating Procedures

STANDARD OPERATING PROCEDURES
Aramis Non Contact Strain Measurement System– Bldg 94

DO NOT use the Aramis unless you have been instructed in its safe use and operation

Appropriate footwear with substantial uppers must be worn.

Use of safety glasses

PRE-OPERATIONAL SAFETY CHECKS

- **Contact authorised user before operation of equipment**
- **Read and familiarise with Aramis operation manual**
- **Use of appropriate PPE**
- **Inspect all electrical cords are tested and current (see label)**
- **Check condition of electrical cords for damage**
- **Read and familiarise with facility/laboratory SSO**
- **Visually inspect equipment for damage**

OPERATIONAL SAFETY PROCEDURES

- **Use correct manual handling practices and lifting equipment where required**
- **Do not point camera mount laser in the direction of any persons**
- **Ensure electrical cords are laid in a manner preventing tripping hazards**
- **Protect equipment from damaging environments (impact, temperature, etc.)**

Post OPERATIONAL PROCEDURES

- **Ensure all electrical items are switched off at the source before removing items from power source**
- **Secure all cords to avoid creating a tripping hazard**
- **Make sure items are clean, wiped with cloth before storing in correct housing**
- **Use correct manual handling practices and lifting equipment where required**

HOUSEKEEPING

- **All items are to be kept in a neat and tidy state and stored neatly.**
- **All items are stored at the owner’s risk. It is an open area.**
- **If in doubt, please contact the OIC or Deputy OIC.**

POTENTIAL HAZARDS

■ **Laser Type 1**	■ **Trip hazards**	■ **Slip hazards**

Page classification: UNCLASSIFIED

DEFENCE SCIENCE AND TECHNOLOGY ORGANISATION DOCUMENT CONTROL DATA	1. PRIVACY MARKING/CAVEAT (OF DOCUMENT)

2. TITLE Optimisation and Validation of the ARAMIS Digital Image Correlation System for use in Large-scale High-strain-rate Events	3. SECURITY CLASSIFICATION (FOR UNCLASSIFIED REPORTS THAT ARE LIMITED RELEASE USE (L) NEXT TO DOCUMENT CLASSIFICATION) Document (U) Title (U) Abstract (U)
4. AUTHOR(S) Vanessa Pickerd	5. CORPORATE AUTHOR DSTO Defence Science and Technology Organisation 506 Lorimer St Fishermans Bend Victoria 3207 Australia

6a. DSTO NUMBER	6b. AR NUMBER	6c. TYPE OF REPORT	7. DOCUMENT DATE
DSTO-TN-1203	AR-015-700	Technical Note	August 2013

8. FILE NUMBER	9. TASK NUMBER	10. TASK SPONSOR	11. NO. OF PAGES	12. NO. OF REFERENCES
2012/1093947/1	NAV 07/359	NAV	31	26

13. DSTO Publications Repository	14. RELEASE AUTHORITY
http://dspace.dsto.defence.gov.au/dspace/	Chief, Maritime Platforms Division

15. SECONDARY RELEASE STATEMENT OF THIS DOCUMENT

Approved for public release

OVERSEAS ENQUIRIES OUTSIDE STATED LIMITATIONS SHOULD BE REFERRED THROUGH DOCUMENT EXCHANGE, PO BOX 1500, EDINBURGH, SA 5111

16. DELIBERATE ANNOUNCEMENT

No Limitations

17. CITATION IN OTHER DOCUMENTS Yes

18. DSTO RESEARCH LIBRARY THESAURUS

ARAMIS; Digital Image Correlation; DIC; blast; high-strain rate

19. ABSTRACT
This document provides an overview for the optimisation of the ARAMIS v6.3.0 digital image correlation system (GOM mbH, Germany) for use in a large-scale, high strain-rate synergistic blast and fragmentation event. The ARAMIS system uses 3D digital photogrammetry to track surface deformation of an object during an event and produces the resultant strain data. This document highlights some key considerations for use of high-speed photogrammerty for synergistic events, not fully covered by the hardware and software manuals or literature.

Page classification: UNCLASSIFIED